Acta Mechanica Solida Sinica, Vol. 22, No. 6, December, 2009 ISSN 0894-9166
Published by AMSS Press, Wuhan, China.

MULTIAXIAL BEHAVIOR OF NANOPOROUS SINGLE CRYSTAL COPPER: A MOLECULAR DYNAMICS STUDY**

Kejie Zhao[1,2] **Liangliang Fan**[1]

[1](*The MOE Key Laboratory, School of Aerospace, Xi'an Jiaotong University, Xi'an* 710049*, China*)

[2](*School of Engineering and Applied Science, Harvard University, Cambridge, Massachusetts* 02138*, USA*)

Changqing Chen[3*]

[3](*Department of Engineering Mechanics, AML, Tsinghua University, Beijing* 100084*, China*)

Received 1 July 2009; revision received 10 October 2009

ABSTRACT The stress-strain behavior and incipient yield surface of nanoporous single crystal copper are studied by the molecular dynamics (MD) method. The problem is modeled by a periodic unit cell subject to multi-axial loading. The loading induced defect evolution is explored. The incipient yield surfaces are found to be tension-compression asymmetric. For a given void volume fraction, apparent size effects in the yield surface are predicted: the smaller behaves stronger. The evolution pattern of defects (i.e., dislocation and stacking faults) is insensitive to the model size and void volume fraction. However, it is loading path dependent. Squared prismatic dislocation loops dominate the incipient yielding under hydrostatic tension while stacking-faults are the primary defects for hydrostatic compression and uniaxial tension/compression.

KEY WORDS molecular dynamics, incipient yield surface, size effect, dislocations, nanoporous single crystal copper

I. INTRODUCTION

Nucleation, growth and coalescence of voids primarily dominate the ductile failure of metals. These three successive processes crucially determine the strength and lifetime of ductile materials. In the past forty years, ductile failure in terms of void growth has been extensively studied from the continuum mechanics standpoints, and a number of classical models have been proposed to quantify the yield criterion and void growth[1–5]. All these continuum models have been proven to be very helpful in understanding the mechanical behaviors of void growth in materials. One issue with the continuum theories is the absence of intrinsic length scale in the constitutive equations and thus is unable to predict the dependence of void growth on void size. However, strong size effects in the sub-micron and nano scales have been repeatly reported in recent investigations[6–10]. In this regard, improved phenomenological theories such as strain gradient theory have been developed to address the size dependence of void

* Corresponding author. Email: chencq@tsinghua.edu.cn

** Project supported by the National Natural Science Foundation of China (Nos.10425210 and 10832002), the National Basic Research Program of China (No.2006CB601202) and the National High Technology Research and Development Program of China (No.2006AA03Z519).

growth[11,12], and the classical continuum models, Gurson model[1] for instance, have been extended to account for the intrinsic length scale effects[13,14].

Moreover, the continuum models do not address the issues related to the geometry of material's microstructure and are not capable of capturing the discrete events (i.e., dislocation emissions) nor revealing the underlying failure mechanism indicating the material yielding. Investigations on dislocation activities around void surfaces under laser shock experiments were conducted in Refs.[6,15]. The experimental results showed clear slip bands nucleated from the grain boundaries in copper. However, direct experimental study of void growth in sub-micron and nano scale (especially the dislocation emission and evolution pattern) is still a formidable task with the current technologies. To better understand the physical pictures of void growth in a metal, a number of numerical simulations have been carried out to capture the dislocation emission and evolution from the void surface. Lubarda et al.[6] demonstrated that the vacancy diffusion mechanism is only valid for low strain rate and/or high temperature cases, and therefore essentially relevant in the creep deformation. Both prismatic dislocation loops and shear dislocation loops have been proposed to dominate the void growth[6–8]. MD simulations conducted by Rudd and co-workers showed the dislocation loops emitted from the void surface resulting in the void expansion. The triaxility effect on the dislocation emission has been studied[16–18]. However, the incipient yield surface and failure mechanisms corresponding to various multi-axial loading modes have not been clarified. In this paper, we report by the molecular dynamics (MD) method that the defect patterns dominating the void growth are loading path dependent. Typically the squared prismatic dislocation loops dominate the incipient yielding of spherical nano-voided copper under hydrostatic tension and stacking faults are the primary defects observed in hydrostatic compression, uniaxial tension/compression cases.

II. SIMULATION METHOD

The multi-axial behavior of nano-sized single crystal Cu with periodic spherical pores is investigated by the Molecular Dynamics (MD) Method. The atomic interaction of Cu in the MD method is modeled by the Embedded Atom Method (EAM) with the potential developed by Foiles et al.[19]. Cubic representative unit cell models are employed in the numerical simulations, where the Cartesian coordinates x, y and z-directions refer to the [100], [010], and [001] crystalline orientations, respectively (see Fig.1). In Fig.1, L denotes the lateral size of the cubic model and R is the radius of the spherical void centered at the model. Accordingly, the void volume fraction is given by

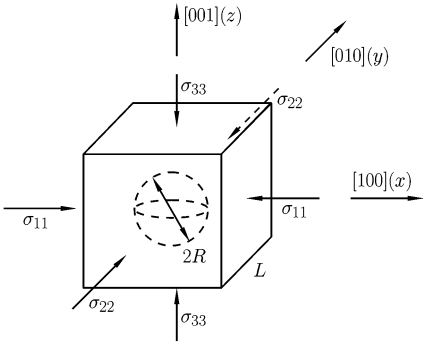

Fig. 1 Schematic of a unit cell of nano-voided copper subject to multi-axial loading.

$$f_v = \frac{4\pi R^3}{3L^3} \tag{1}$$

The model is subject to multi-axial loading (i.e., σ_{11}, σ_{22} and σ_{33}). During the loading process, $\sigma_{11} = \sigma_{22}$ is enforced to mimic the axisymmetric loading state. Before imposing the loading, the atomic systems are relaxed with the conjugate gradient method to reach the minimum energy state. In all simulations, suitable strains are applied to impose the multi-axial stressing. By changing the applied strain ratio along [100] and [001] directions (i.e., $\varepsilon_{11}/\varepsilon_{33}$), different loading modes could be obtained. In the study, a maximum of 0.05% strain increment is adopted in each loading step. Furthermore, numerical results show that the strain rate $\dot{\varepsilon} = 1 \times 10^8$ s^{-1} is a good trade-off between computational efficiency and unexpected strain rate effects in MD simulation and is used throughout this study. The system temperature is controlled to be around 0K during loading to avoid thermal activation. Simulations reported are performed by using the large-scale atomic/molecular massively parallel simulator (LAMMPS)[20]. Defected atomistic configurations during deformation were viewed by using ATOMEYE[21].

III. RESULTS AND DISCUSSIONS

One of the main objectives is to study the defect evolution pattern during the multi-axial loading. The centrosymmetry parameter P defined by Kelchner et al.[22] is appropriate to illustrate various defects in FCC single crystals (e.g., partial dislocation, stacking fault, and surface atom) and is adopted to show the loading induced defect evolution. For each atom in a FCC single crystal, its centrosymmetry parameter is defined as

$$P = \sum_i |\boldsymbol{R}_i + \boldsymbol{R}_{i+6}|^2 \tag{2}$$

where $\boldsymbol{R}_i$ and $\boldsymbol{R}_{i+6}$ are the vectors corresponding to the six pairs of opposite nearest neighbors in the FCC lattice. Thus, $P = 0$ represents the undisturbed state of the perfect lattice, and P will increase for any defects and for atoms close to free surfaces. In the case of single crystal copper, $0.5 < P < 3$ corresponds to partial dislocation, $3 < P < 16$ for stacking faults, and $P > 16$ for surface atoms.

3.1. Incipient Yield Surface

Figure 2(a) shows the MD simulated hydrostatic stress-volume strain curve of nano-porous single crystalline copper under hydrostatic tension. The void volume fraction is 22% and model size is $L = 24a_0$ and $a_0 = 0.3615$ nm is the lattice constant of copper. It is found that the stress drops abruptly at about 6.8 GPa (labeled as point A in the insert). The atomic system gains its strength again with the strain increasing further, until reaching its peak strength of 8.9 GPa. Examination of the atomic structures with the defined centrosymmetry parameter P reveals that, prior to point A, the centrosymmetry parameter during loading is close to zero everywhere except for the surface atoms. With one loading increment beyond point A (i.e., point B in the insert), however, partial dislocations start to initiate. The observation is illustrated in Figs.2(b) and (c) for the atomic configurations at points A and B, respectively, where only atoms with $P > 0.5$ are visible. In fact, the atomic configurations from the very beginning until point A are very similar and only that for point A is shown for illustration purpose. Figure 2(b) indicates that the system maintains its nearly perfect atomic structure until point A whilst Fig.2(c) shows that the system starts to lose its perfect structure, resulting in defect evolution (i.e., dislocations emission). This fact rationalizes the definition of the stress at point A as the incipient yield stress. It should be pointed out that the incipient yield point can be uniquely defined for any other multi-axial loadings. After initiation, dislocations meet and form sessile junctions which subsequently change the shape of evolving loops. Interactions between dislocations lead to enhanced dislocation density around the void surface and working hardening of the material. This may partly explain why the system re-gains its strength beyond point B until reaching its peak.

Systematical multi-axial simulations are conducted for different loading paths with various values of σ_{33}/σ_{11} ($\sigma_{11} = \sigma_{22}$). The corresponding incipient yield stress can be identified from the simulated

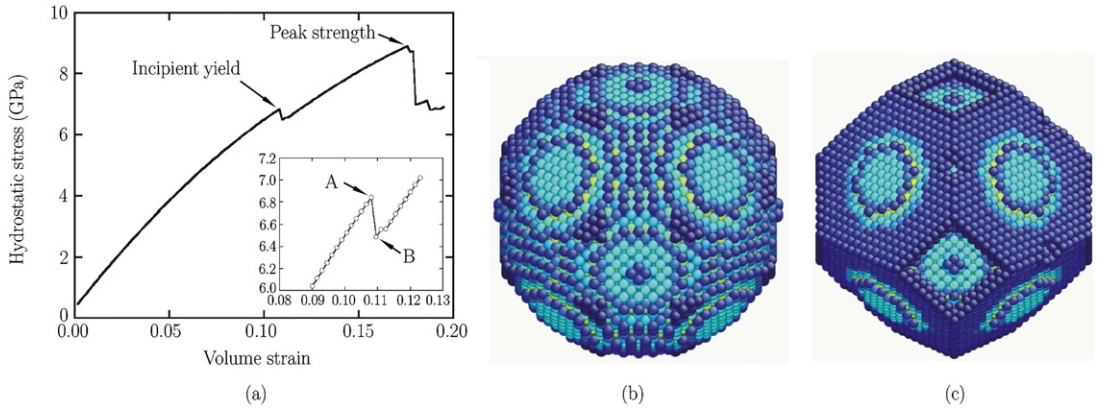

Fig. 2. (a) Stress-strain response curve for spherical nano-voided copper under hydrostatic tension, and the associated enlarged view of the incipient yielding stage; (b) Atomistic configuration corresponding to point A (the incipient yield point); (c) Defected atomistic configuration corresponding to point B. (Atoms are colored by their centrosymmetry parameter, and only atoms with the centrosymmetry parameter larger than 0.5 are visible.)

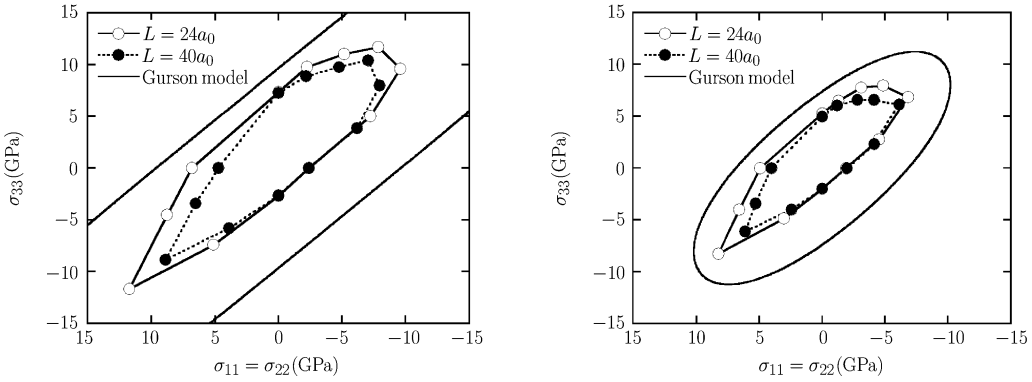

Fig. 3. MD predicted incipient yield surface in the σ_{11}-σ_{33} space of nanoporous single crystalline copper.

stress-strain curves in conjunction with the evolution of the atomic configurations. Figures 3(a) and (b) show the calculated incipient yield surfaces (denoted by symbols) in the σ_{11}-σ_{33} space for nano-porous single crystal Cu with void volume fractions of 0.82% and 22%, respectively. In Fig.2, two model sizes are considered (i.e. $L = 24a_0$ and $L = 40a_0$). In Fig.3, the Gurson model[1] is also included as solid lines for comparison. Note the Gurson model is given by

$$\Phi = \frac{\sigma_e^2}{\sigma_y^2} + 2f_v \cosh\left(\frac{\sigma_{kk}}{2\sigma_y}\right) - 1 - f_v^2 = 0 \tag{3}$$

where σ_e is the macroscopic equivalent von Mises stress, σ_{kk} represents the dilatational stress and σ_y is the yield stress of the solid material. For ideal single crystalline copper without defects, the uniaxial yield stress can be approximated as $\sigma_y \approx G/5 = 9.74$ GPa, with $G = 48.7$ GPa being the shear modulus.

It is seen from Fig.3 that the MD predictions differ significantly from Gurson's continuum model: The yield surfaces given by MD simulations are asymmetric in tension and compression and are void size dependent for a given void volume fraction, showing smaller voids behave stronger. However, the Gurson model is symmetric about tension and compression and is void size independent. The void size independency of the Gurson model is apparent by noting that no intrinsic length scale is present in Eq.(3).

From Fig.3(a), it is found that the Gurson model for the case of $f_v = 0.82\%$ is close to the von Mises material yield criterion. However, the simulation result shows the incipient hydrostatic strength is comparable to that under uniaxial loading, even when the void volume fraction is very small (i.e. $f_v = 0.82\%$). This difference may be attributed to the isotropic nature of the Gurson model while the model in this study is cubic single crystal material copper which is anisotropic. In Fig.3(b), the Gurson model is seen to be significantly larger than those predicted by the MD simulations. Comparison of the MD predicted incipient yield surfaces in Figs.3(a) and (b) show that the incipient yield surfaces for different void volume fractions are geometrically self-similar.

3.2. Void Size Effects on Incipient Yielding Strength

In Fig.3, apparent size effects on the incipient yield surfaces are observed: smaller voids generally behave stronger in terms of the yielding strength. To explore the size effects further, we have simulated the hydrostatic incipient yield strength by fixing the void volume fraction of $f_v = 0.82\%$ and varying the sample size from $L = 24a_0$ to $L = 64a_0$. The biggest sample contains 1,039,987 atoms. The MD predicted size dependency of the hydrostatic incipient yield strength upon the void size is shown in Fig.4 as symbols, where G is the shear modulus and b is the Burgers vector. For $\{111\}\langle 110\rangle$ dislocation in FCC single crystal copper, the magnitude of the Burgers vector is 0.255 nm. It is clear from Fig.4 that the yield stress decreases with increasing R/b. Lubarda et al.[6] developed a dislocation based model to account for the size effect in the yield strength of voided solids,

$$\frac{\sigma_{\rm cr}}{G} = \frac{b/R}{\sqrt{2}\pi(1-\nu)} \frac{(1+\sqrt{2}R_{\rm core}/R)^4 + 1}{(1+\sqrt{2}R_{\rm core}/R)^4 - 1} \tag{4}$$

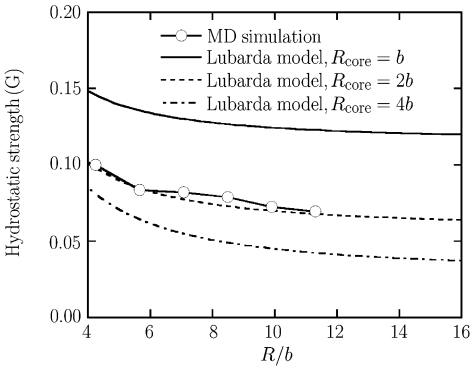

Fig. 4. Void size effect on the incipient yield strength under hydrostatic tension. The void volume fraction is $f_v = 0.82\%$.

where σ_{cr} is the yield stress, G the shear modulus, b the Burger's vector, R the initial void radius, ν the Poisson's ratio (taken as 0.3 in this paper), and R_{core} is the dislocation core radius. Predictions of Eq.(4) with $R_{core} = b$, $2b$, and $4b$ are shown in Fig.4 as lines. It can be found that the model by Lubarda et al. with $R_{core} = 2b$ agrees well with the present atomic simulation. Moreover, the present results are also consistent with Ref.[7], which also shows that the size effect in laser shock simulation agrees with Eq.(4) using $R_{core} = 2b$.

3.3. Failure Mechanism Associated with Various Loading Modes

The material inherent and loading induced defects are believed to have important roles in dictating the material properties, especially the strength. In MD simulations, it is possible to examine the defect evolution pattern associated with the loading process, which may shed insightful light on the underlying mechanism of the failure of materials. To this end, the atomic configurations and defect patterns associated with various multi-axial loadings are visualized and identified by employing centrosymmetry parameters[22] and open-source software ATOMEYE[21]. Figure 5 shows the dislocation emission from the void free surface of a model ($L = 24a_0$ with $f_v = 22\%$) under hydrostatic tension. Only atoms with their centrosymmetry parameters in the range $0.5 < P < 3$ are shown. It is seen that six symmetric prismatic dislocation loops are induced at the incipient yielding, which implies the onset of plastic deformation induced by hydrostatic tension. The dislocation loops are composed of four edges laid in FCC single crystal slip plane {111}. Interestingly, the shape of the predicted loops is not an arc. This may be due to the fact that the local value of the line tension varies with orientation in anisotropic materials[23]. As a consequence, the shapes of dislocation loops observed in experiments for anisotropic materials are more likely to be polygon(e.g., square, hexagon) instead of circles in isotropic materials.

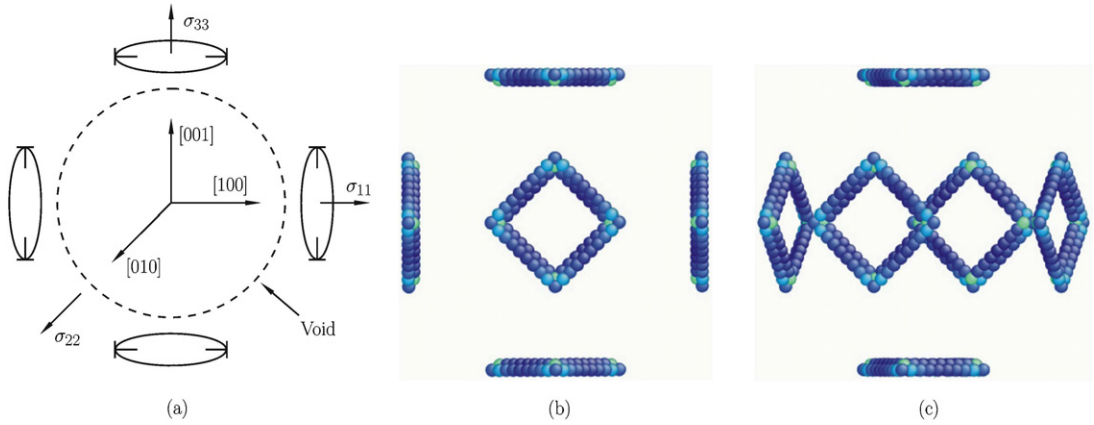

Fig. 5. (a) Schematic of prismatic dislocation loops around the void under macroscopically applied multiaxial stressing; (b) Predicted prismatic dislocation loops at the incipient yield point; (c) Side view of the dislocation loops. (Only atoms with centrosymmetry parameters in the range $0.5 < P < 3$ are shown. The model is of size $L = 24a_0$ with $f_v = 22\%$.)

Figure 5 confirms the theoretical prediction[8] that prismatic dislocation loop emissions dominate the ductile failure of metals under hydrostatic loading.

The defected atomic configurations for three loading modes (i.e., hydrostatic compression and uniaxial tension/compression) of the same model are plotted in Fig.6. It can be seen that the stack-fault defects dominate the three plastic deformations. Further examination shows that four faces of FCC single crystal {111} slip planes constitute the tetrahedron in Figs.6(b) and (c). Each face of the tetrahedron is a stacking-fault zone intersecting with the edges of Lomer-Cottrell dislocations. Also, the cross section of the tetrahedron is empty, which implies its interior is the region of perfect atoms. Therefore, the tetrahedron is a typical stack-fault tetrahedron, a common vacancy-type cluster of FCC single crystals. The atomic configurations at the incipient yield have also been investigated for different model sizes and void volume fractions. It is found that the partial dislocation loops and stacking faults dominate the incipient yielding of nano-porous single crystalline copper subject to multi-axial loading, and the defect evolution patterns are sensitive to the loading path. However, the defect patterns for different void volume fractions but the same sample size are almost identical.

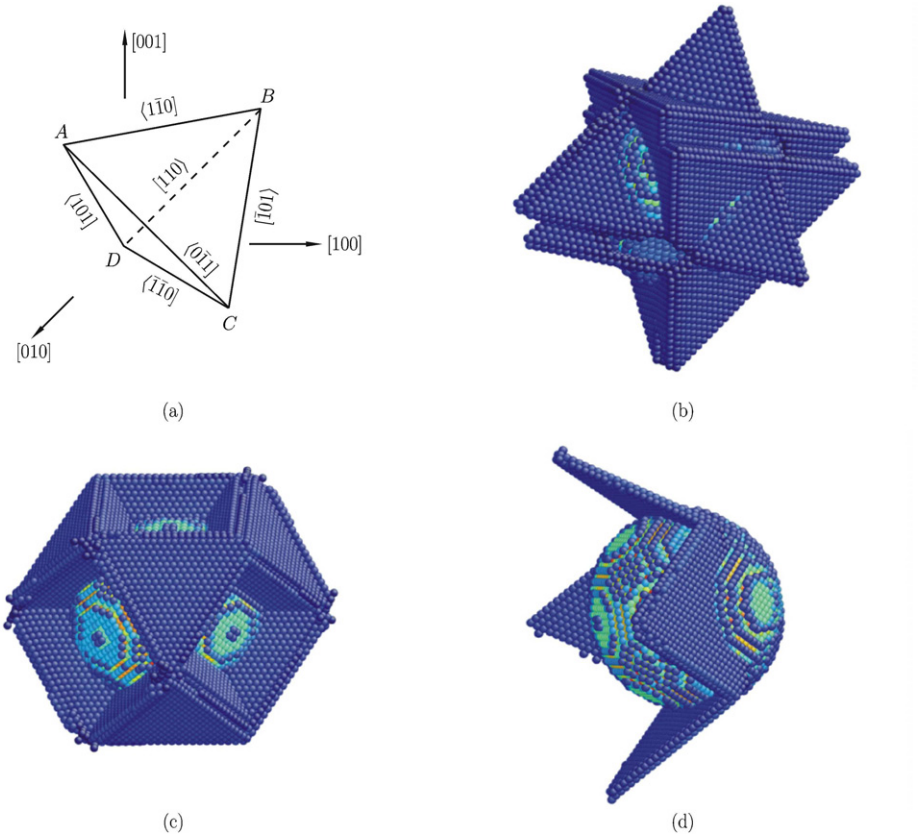

Fig. 6. (a) Schematic of FCC single crystal slip systems in a Thompson tetrahedron. Atomic defect configurations of nano-voided copper at the incipient yield point under (b) hydrostatic compression, (c) uniaxial tension, and (d) uniaxial compression. (Only atoms with their centrosymmetry parameters larger than 0.5 are visible. The model is of size $L = 24a_0$ with $f_v = 22\%$.)

IV. CONCLUSIONS

The multi-axial stress-strain response and incipient yield surfaces of nano-porous single crystalline copper are investigated by the MD method. The underlying deformation mechanism and defect evolution patterns are explored. It is found that the discrete event of partial dislocation emission (i.e., the incipient plasticity) corresponds to abrupt drop in the associated stress-strain response curves.

The incipient yield surfaces are asymmetric in tension-compression and are geometrically self-similar for different void volume fractions but the same model size. Size effects are predicted in the incipient yield surface for a given void volume fraction: the smaller behaves stronger. Failure mechanisms accompanying different loading modes are studied. It is found that the defect pattern is sensitive to the multi-axialloading path. Specifically, the squared prismatic dislocation loops dominate the incipient yielding under hydrostatic tension while stack-faults are the prime defects for hydrostatic compression and uniaxial tension/compression. However, the defect patterns are insensitive to the sample size and the void volume fraction.

References

[1] Gurson,A.L., Continuum theory of ductile rupture by void nucleation and growth — 1. Yield criteria and flow rules for porous ductile media. *Journal of Engineering Materials and Technology-Transactions of the Asme*, 1977, 99(1): 2-15.

[2] McClinto,F.A., A criterion for ductile fracture by growth of holes. *Journal of Applied Mechanics*, 1968, 35(2): 363-371.

[3] Rice,J.R. and Tracey,D.M., On ductile enlargement of voids in triaxial stress fields. *Journal of the Mechanics and Physics of Solids*, 1969, 17(3): 201-217.

[4] Tvergaard,V., Influence of voids on shear band instabilities under plane-strain conditions. *International Journal of Fracture*, 1981, 17(4): 389-407.

[5] Needlema,A., Void growth in an elastic-plastic medium. *Journal of Applied Mechanics-Transactions of the Asme*, 1972, 39(4): 964-970.

[6] Lubarda,V.A., Schneider,M.S., Kalantar,D.H., Remington,B.A. and Meyers,M.A., Void growth by dislocation emission. *Acta Materialia*, 2004, 52(6): 1397-1408.

[7] Davila,L.P., Erhart,P., Bringa,E.M., Meyers,M.A., Lubarda,V.A., Schneider,M.S., Becker,R. and Kumar,M., Atomistic modeling of shock-induced void collapse in copper. *Applied Physics Letters*, 2005, 86(16): 161902.

[8] Ahn,D.C., Sofronisa,P. and Minich,R., On the micromechanics of void growth by prismatic-dislocation loop emission. *Journal of the Mechanics and Physics of Solids*, 2006, 54(4): 735-755.

[9] Traiviratana,S., Bringa,E.M., Benson,D.J. and Meyers,M.A., Void growth in metals: Atomistic calculations. *Acta Materialia*, 2008, 56(15): 3874-3886.

[10] Huang,M.S., Li,Z.H. and Wang,C., Discrete dislocation dynamics modelling of microvoid growth and its intrinsic mechanism in single crystals. *Acta Materialia*, 2007, 55(4): 1387-1396.

[11] Fleck,N.A. and Hutchinson,J.W., Strain gradient plasticity. *Advances in Applied Mechanics*, 1997, 33: 295-361.

[12] Liu,B., Qiu,X., Huang,Y., Hwang,K.C., Li,M. and Liu,C., The size effect on void growth in ductile materials. *Journal of the Mechanics and Physics of Solids*, 2003, 51(7): 1171-1187.

[13] Wen,J., Huang,Y., Hwang,K.C., Liu,C. and Li,M., The modified Gurson model accounting for the void size effect. *International Journal of Plasticity*, 2005, 21(2): 381-395.

[14] Li,Z.H. and Steinmann,P., RVE-based studies on the coupled effects of void size and void shape on yield behavior and void growth at micron scales. *International Journal of Plasticity*, 2006, 22(7): 1195-1216.

[15] Meyers,M.A. and Aimone,C.T., Dynamic fracture (spalling) of metals. *Progress in Materials Science*, 1983, 28(1): 1-96.

[16] Seppala,E.T., Belak,J. and Rudd,R.E., Onset of void coalescence during dynamic fracture of ductile metals. *Physical Review Letters*, 2004, 93(24): 245503.

[17] Seppala,E.T., Belak,J. and Rudd,R.E., Effect of stress triaxiality on void growth in dynamic fracture of metals: A molecular dynamics study. *Physical Review B*, 2004, 69(13): 134101.

[18] Seppala,E.T., Belak,J. and Rudd,R.E., Three-dimensional molecular dynamics simulations of void coalescence during dynamic fracture of ductile metals. *Physical Review B*, 2005, 71(6): 064112.

[19] Foiles,S.M., Baskes,M.I. and Daw,M.S., Embedded-atom-method functions for the Fcc metals Cu, Ag, Au, Ni, Pd, Pt, and their alloys. *Physical Review B*, 1986, 33(12): 7983-7991.

[20] Plimpton,S., Fast parallel algorithms for short-range molecular-dynamics. *Journal of Computational Physics*, 1995, 117(1): 1-19.

[21] Li,J., AtomEye: an efficient atomistic configuration viewer. *Modelling and Simulation in Materials Science and Engineering*, 2003, 11(2): 173-177.

[22] Kelchner,C.L., Plimpton,S.J. and Hamilton,J.C., Dislocation nucleation and defect structure during surface indentation. *Physical Review B*, 1998, 58(17): 11085-11088.

[23] Dewit,G. and Koehler,J.S., Interaction of dislocations with an applied stress in anisotropic crystals. *Physical Review*, 1959, 116(5): 1113-1120.